

Effects of *p*-Hydroxybenzoic Acid Monomer Units on Physical Properties of Thermal Liquid Crystalline Poly(ester imide ketone)s

Jun Xu,¹ Yafei Zhu,² Yi Zhang,¹ Yimin Zheng,¹ Zhenguo Chi,¹ Jiarui Xu¹

¹Key Laboratory for Polymeric Composite and Functional Materials of Ministry of Education, Materials Science Institute, School of Chemistry and Chemical Engineering, Sun Yat-sen (Zhongshan) University, Guangzhou 510275, China

²Instrumental Analysis and Research Center, Sun Yat-sen (Zhongshan) University, Guangzhou 510275, China

Received 18 February 2006; accepted 1 June 2006

DOI 10.1002/app.25504

Published online in Wiley InterScience (www.interscience.wiley.com).

ABSTRACT: A series of poly(ester imide ketone)s (PEIKs) with varied *p*-hydroxybenzoic acid (HBA) molar fraction derived from *N,N'*-hexane-1,6-diylbis(trimellitimide), 4,4'-dihydroxybenzophenone, and *p*-hydroxybenzoic acid were synthesized by a "step-feeding" polycondensation method in benzene sulfonyl chloride, dimethylformamide, and pyridine. High field ¹H, ¹³C, and 2D NMR spectroscopy measurements were combined to determine the assignments of hydrogen and carbon atoms in the copolymers. ¹³C inverse gated decoupling NMR spectra were taken and used as a quantitative method to analyze the chain sequence structures of these copolymers. The liquid crystalline behaviors and thermal properties of the PEIKs were characterized by polarized light microscopy (PLM), wide-angle X-ray diffraction (WAXD), differential scanning calorimetry (DSC), and thermogravimetric analysis (TGA). The NMR studies show that the monomeric unit ratios of the PEIKs are very close to the ratios of the monomers

added into the polycondensation process. The analytical results of sequence distribution indicate that the sequence ratios of I-H, H-D, and H-H dias rise with the increase of HBA molar fraction, while that of I-D decrease. It is worth noting that the sequence ratios of H-H are always very small among the four sequence ratios although the HBA molar fraction varied from 0 to 50%. It was shown that the copolymers possess a typical nematic thermotropic liquid crystalline character and high thermal stability, which is strongly related with the changes in sequence structure of the molecular chains. This type of liquid crystalline polymers also exhibits excellent fiber-forming character in the melting state, which would find its potential usages in high performance fiber and fiber modification materials. © 2006 Wiley Periodicals, Inc. *J Appl Polym Sci* 103: 3183–3193, 2007

Key words: poly(ester imide ketone); thermotropic liquid crystalline polymer (TLCP); NMR; sequence structure

INTRODUCTION

Thermotropic liquid crystalline poly(ester imide)s (TLCPEIs) have attracted great attention since 1987, when poly(ester imide) (PEI) with thermotropic liquid crystalline character was first synthesized by Kricheldorf and Pakull.¹ Up to now, a wide variety of PEIs and TLCPEIs have been synthesized, especially those with a regular sequence of rigid rod-like aromatic imide "mesogenic" units and flexible "spacer" units, and their properties as well as liquid crystalline behaviors have been well characterized.^{2–8}

Yet, to the best of our knowledge, nearly all the reported PEIs with higher molecular weight were synthesized by the melt transesterification approach at high temperature under decompression.⁹ This might be practical from an industrial standpoint, but is quite complicated for fundamental investigations of such aspects as the reaction mechanism and the relations of sequence structure and properties of the copolymers. As been well known, the physical and mechanical properties of a thermotropic liquid crystalline polymer (TLCP) are mainly determined by its molecular structures, including chemical composition, chain sequence structures, molecular weight, and molecular weight distribution. So it is very important to develop a feasible approach to synthesize PEIs with well-designed chemical composition and chain sequence structures. An ameliorated direct so-

Correspondence to: J. Xu (xjr@mail.sysu.edu.cn).

Contract grant sponsor: National Natural Science Foundation of China; contract grant number: 50473020.

Contract grant sponsor: Ministry of Education of China; contract grant number: 20050558001.

Contract grant sponsor: Department of Science Technology of Guangdong Province; contract grant number: 2004A10703001.

Contract grant sponsor: Sun Yat-sen University.

lution polycondensation method, which is based on the method ever developed by Higashi and his coworkers for the purpose of copolyesters synthesis,^{10,11} to synthesize TLCPEIs was developed in our laboratory with tosyl chloride (TsCl) in pyridine (Py) by dimethyl formamide (DMF) catalyzed alcoholysis.¹²

Nevertheless, during the copolymerization process a major problem to control the chain sequence exists, that some monomers with two different function groups, such as *p*-hydroxybenzoic acid, cannot only copolymerize with other monomers but also self-polymerize. In addition, under certain conditions, the difference of the relative reactivity of the function groups in the monomers usually results in competitive reactions. Even for the same type of monomers, the resultant products may be a random copolymer, an alternate copolymer or a block copolymer, or their mixture, resulting in variable properties for the final copolymers. To study the effects of the distribution of rigid and flexible segments on the properties of PEIs in detail, it is necessary to look into the chain sequence structures of the polymers with assurance.

In our previous publication, a series of PEIKs from *N,N'*-hexane-1,6-diylbis(trimellitimide) (IA6), 4,4'-dihydroxybenzophenone (DHBP), and *p*-hydroxybenzoic acid (HBA) were prepared by a so-called two-step reaction.¹³ That is, the IA6 monomer was activated by condensing agent first, and then Py solution of mixed HBA and DHBP was added dropwise. However, it was found that the sequence structures of the resultant PEIKs could not be well controlled. In this present article, all the PEIKs were prepared by a modified three-step-feeding polycondensation process. In this process, IA6 was first activated by condensing agent, followed by adding the HBA/Py solution and then the DHBP/Py solution. Through this means, we anticipate that the IA6 monomers would fully react with HBA in these two steps. In the next step, the resultant from the former steps was polymerized with the DHBP monomer, and PEIK was obtained in the end. During the whole copolymerization process, the reactions were well controlled by the reaction temperature and time as well as the feed-in speed of the monomers. Subsequently, the sequence structures of the resultant polymers were determined by high-field nuclear magnetic resonance spectroscopy (NMR), and the properties of the copolymers were characterized by PLM, DSC, TGA, and WAXD. The effects of HBA monomeric unit ratios as well as the molar fraction of different rigid and soft sequences in the polymer chains on the TLC properties of PEIKs were discussed, which has not yet been reported in detail in the literature.

EXPERIMENTAL

Materials

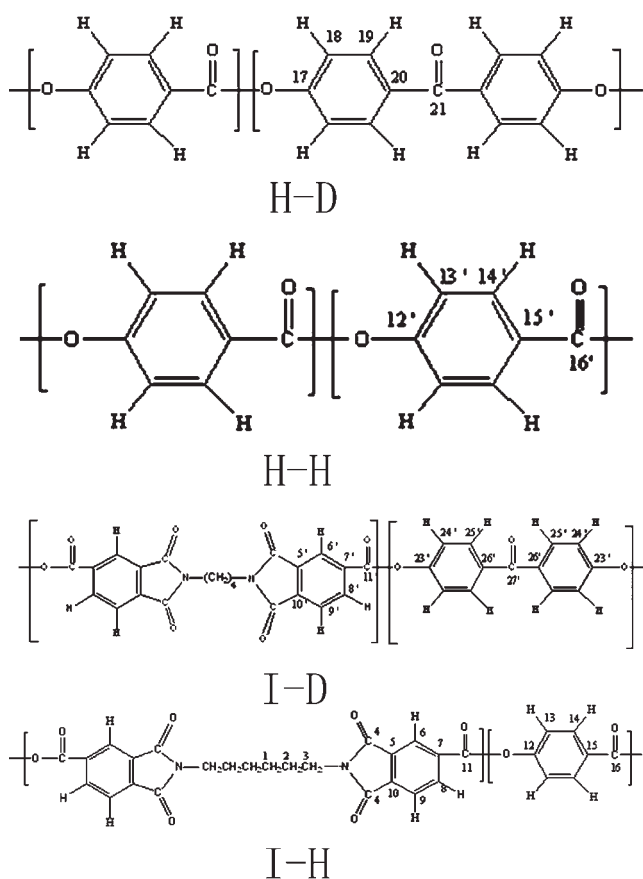
N,N'-Hexane-1,6-diylbis(trimellitimide) was synthesized from trimellitic anhydride and 1,6-hexane diamine according to the method detailed by Kricheldorf et al.³ Synthesis of 4,4'-dihydroxybenzophenone from phenol and *p*-hydroxybenzoic acid is according to the method of Stanley.¹³ Pyridine was purified by distillation over sodium hydroxide. Other materials were obtained as chemical grade reagents from a commercial source (Guangzhou Medicine Company, Guangzhou, China) and used as received.

Condensation

About 3.32 mL (0.026 mol) of benzene sulfonyl chloride (BsCl), 1.55 mL (0.020 mol) of dimethylformamide (DMF), and 10 mL of pyridine (Py) were put into a 250 mL one neck round bottom flask with an electromagnetic stirrer. The mixture was aged at room temperature for 30 min. Then, 5 mmol of *N,N'*-hexane-1,6-diylbis(trimellitimide) was added into the flask under stirring. After the resulting mixture became solidified, the flask was placed into an oil bath preheated to 80°C and was maintained for 10 min. Then 5–10 mL of Py solutions containing 0–10 mmol of *p*-hydroxybenzoic acid were added to the above mixture all in once. After the above resultant was maintained for 30 min, 10 mL Py solution of 4,4'-dihydroxybenzophenone (5 mmol) was added dropwise for 10 min. The temperature was maintained at 80°C for 3 h. After dilution with 20 mL of DMF, the precipitate was filtered and washed with alcohol. The resultant polymers were dried in a far-infrared oven.

Measurements

All NMR spectra were recorded at room temperature on a Varian Unity Inova 500 NB spectrometer, operating at 499.774 MHz for ¹H with indirect detection probe and at 125.682 MHz for ¹³C with broadband probe. Samples were made up as solution of ~ 10–20 mg of each polymer in 0.7 mL of deuterated trifluoroacetic acid (CF₃COOD), using tetramethylsilane (TMS) as the internal reference. Inverse gated decoupling was exploited for quantitative carbon nuclei intensities, using a 24° pulse angle, 0.45 s acquisition time, and 2.0 s relaxation delay for about 5000 scans. Two-dimensional spectra were performed by using standard Varian software and the parameters used were as follows: COSY spectra were collected with four transients for each 256 increments and the spectral windows were 4096.5 Hz in both dimensions. HMQC spectra were recorded



Scheme 1 The possible monomer connecting manners.

with spectral windows of 4096.5 Hz in f_2 and 14,842.3 Hz in f_1 , collected with 16 transients for each 256 increments. HMBSC spectra were recorded with spectral windows of 4096.5 Hz in f_2 and 23,619.7 Hz in f_1 , collected with 24 transients for each 128 increments.

The liquid crystalline texture of the resultant polymers were observed under a Leitz Orthoplan optical microscope equipped with cross-polarizers and a hot stage.

Differential scanning calorimetry (DSC) measurements were conducted with TA Instruments MDSC 2910 under nitrogen purge and the scanning rate used was 20°C/min.

The wide-angle X-ray diffraction curves (WAXD) were measured with a Rigaku XD-3A diffractometer using Ni-filtered Cu K α radiation and $\lambda = 1.54$ Å. Samples were prepared in the form of powder. The diffractograms were recorded in 2θ range between 5 and 60° at a rate of 5°/min.

Thermogravimetric analysis (TGA) was performed in air using Shimadzu TGA-50H at a heating rate of 20°C/min.

RESULTS AND DISCUSSION

As described in the Experimental section, the materials were added in the following sequence: first, *N,N'*-hexane-1,6-diylbis(trimellitimide) (IA6) was activated by BsCl/DMF/Py mixed condensing agent; next, certain amount of *p*-hydroxybenzoic acid (HBA) ranging from 0 to 50% molar fraction to total was added; last, the same molar fraction of 4,4'-dihydroxybenzophenone (DHBP) as that of IA6 was added into the reactive system. With this monomer feeding method, there are only four possible polycondensation reaction manners between any two monomers in the system, as shown in Scheme 1. Products with 0, 10, 20, 33, 40, and 50% molar fraction of HBA are designated, referred to below as PEIK(A–F), respectively.

For convenience in discussion, these four kinds of connecting sequences are abbreviated as I–H, I–D, H–H, and H–D. The carbon atoms in each sequence unit are also numbered for assignment.

$^1\text{H-NMR}$ predominant intensity signals assignment

Figure 1 shows the full range $^1\text{H-NMR}$ spectrum for PEIK(F) dissolved in CF_3COOD . Most signals were assigned based on well-known proton NMR chemical shift displacements resulting from electron shielding/deshielding of the hydrogen nuclei by the inductive effects, or from the diamagnetic anisotropy of various neighboring functional groups.

In the IA6 monomeric unit, the positions of protons H-1 (1.60 ppm), H-2 (1.90 ppm), and H-3 (3.94–3.97 ppm) are assigned by their distance leaving the trimellitimide. Among the aromatic protons of IA6, only H-6 (8.89 ppm) shows a single peak because it has no coupling with other *ortho*-benzene protons, and shifts to higher frequency for its 3-bond coupling with C-4 (172.25 ppm) and C-11 (167.59 ppm) which is in the carbonyl of trimellitimide and ester

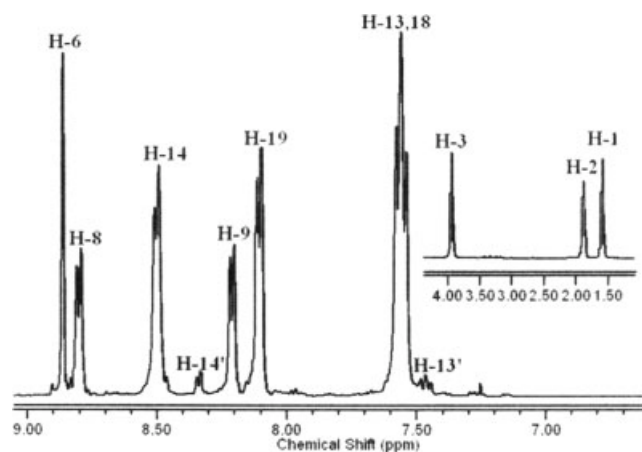


Figure 1 $^1\text{H-NMR}$ spectrum of PEIK(F) in CF_3COOD .

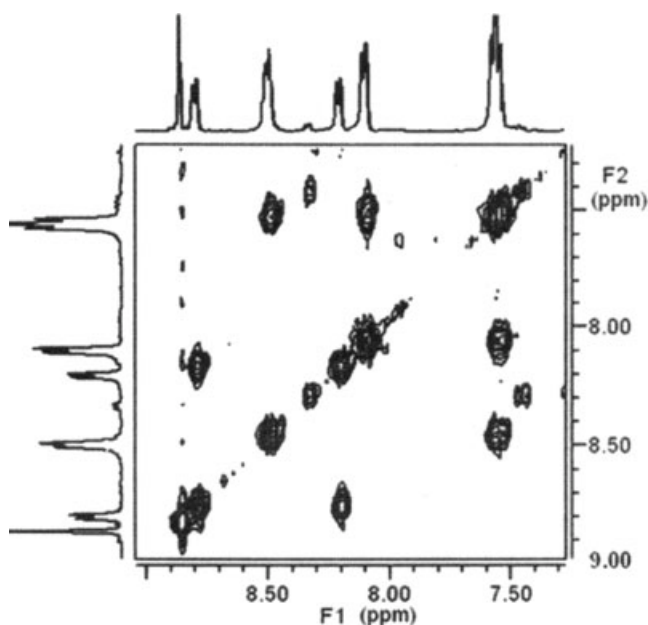


Figure 2 ^1H - ^1H COSY spectrum of PEIK(F) in CF_3COOD .

group, respectively, as shown in Figure 4. C-4 also has a 3-bond coupling with H-9 (8.22–8.23 ppm) besides H-6, so the position of H-9 is assigned. The ^1H - ^1H correlation (COSY) of PEIK(F) in CF_3COOD is shown in Figure 2, and reveals the position of H-8 (8.81–8.83 ppm) through a 3-bond coupling with H-9. In the sequences of I-H and I-D, the positions of protons in IA6 monomeric unit have no obvious change.

Among the carbon atoms in the carbonyl groups, the one in carbonyl group of ketone has higher chemical shift value than it does both in trimelliti-

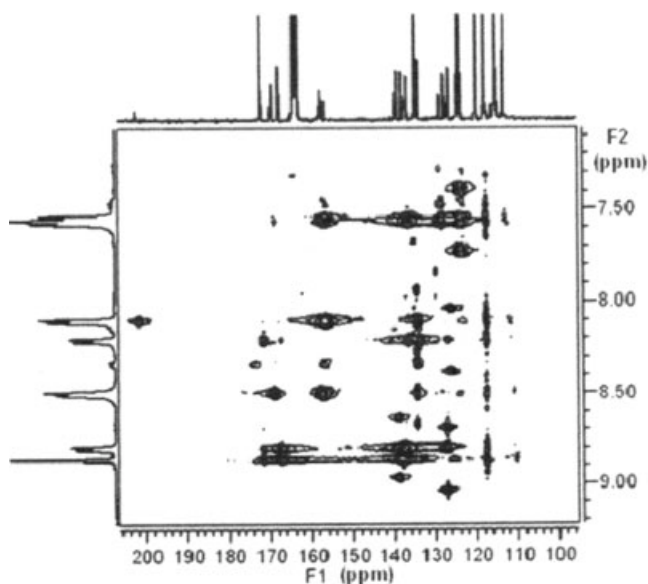


Figure 3 A section of HMBC spectrum of PEIK(F) in CF_3COOD .

mide and ester group (C-21, 202.4 ppm). In the sequence of H-D, assignment of H-19 (8.12–8.13 ppm) was determined by HMBC spectrum of ^{13}C - ^1H correlation spectroscopy with $^3J_{\text{C-H}}$ (7.5 Hz) as shown in Figure 3, which shows a 3-bond coupling from it with already assigned C-21, and assigned the position of its neighbor proton H-18 from ^1H - ^1H COSY (as shown in Fig. 2). But there are three intensive peaks at the position where there should be two peaks for H-18 which has only one neighbor proton of H-19, according to the ^1H couple-split principle. Also observing from the integral value, it could be presumed that there must be other peaks of ^1H with the same chemical shift value of H-18, which will be discussed later.

In the sequences of I-H and H-H, for the resemblance of their ester group, there is little difference between the chemical shifts of their carbon atoms in carbonyl groups from ^{13}C -NMR (C-16, 169.44 ppm; C-16', 169.56 ppm). The positions of H-14 (8.51–8.53 ppm) and H-14' (8.35–8.37 ppm) are determined from the 3-bond correlation of C-16-H-14 and C-16'-H-14'. So does the positions of H-13 and H-13' (7.46–7.48 ppm) which is located at the ortho position of H-14 and H-14', respectively, according to the ^1H - ^1H COSY. The fact proves that the position of H-13 overlaps with H-18 (H-13, 18; 7.56–7.60 ppm).

Other protons like H-18' and H-19' might be too weak or overlap with other intensive peaks. Therefore, their positions are not detectable from the ^1H -NMR spectrum or ^1H - ^1H COSY.

^{13}C -NMR predominant intensity signals assignment

Figure 4 shows the full range ^{13}C -NMR spectrum (inverse gated decoupling) with signal assignments for PEIK(F) dissolved in CF_3COOD . The carbon signals were assigned using well-known carbon chemi-

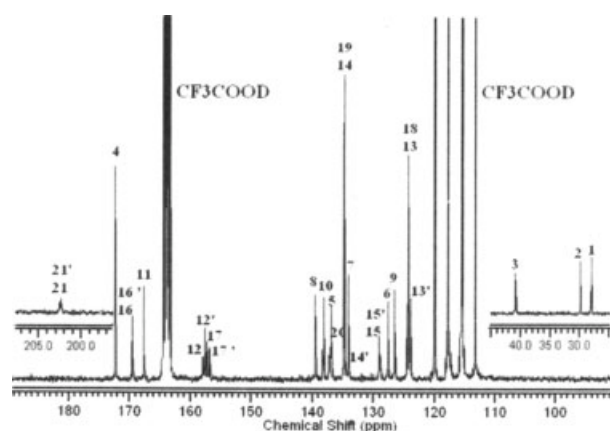


Figure 4 ^{13}C -NMR spectrum (inverse gated decoupling) of PEIK(F) dissolved in CF_3COOD .

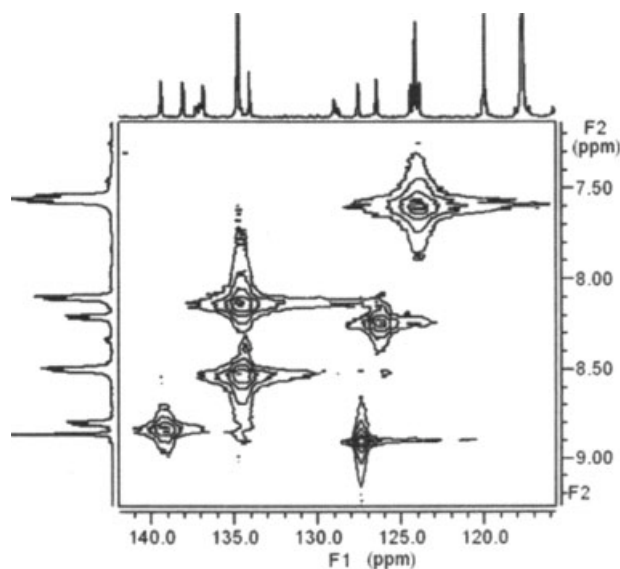


Figure 5 A section of HMQC spectrum of PEIK(F) in CF_3COOD .

cal shifts displacement as well as HMBC and HMQC spectra of ^{13}C - ^1H correlation spectroscopy, respectively, as shown in Figures 3 and 5.

In the earlier section, the positions of some carbon atoms have been assigned using HMBC spectrum of ^{13}C - ^1H correlation spectroscopy. Here, it is continuously adopted to determine the positions of other carbon atoms. Those carbon atoms which are one-bond connecting with proton can also be indicated with HMQC spectrum of ^{13}C - ^1H correlation.

For the accurateness of integration, it was decided to set the integration of the signal C-1 (28.01 ppm) in IA6 monomeric unit to the value of 10.00 because they were in the very center of IA6 monomeric unit and the change of chemical environment could have little effect on their chemical shifts. Table I summarized the peak assignments and integral values of major carbon atoms in PEIK(F).

Determination of monomer ratios and sequence distribution

For the unification and exactness of integration, a same method of integration was used for all the samples, and for the convenience of exemplification, PEIK(F) was taken as an example. Here I is the abbreviation for integration.

As for the monomeric unit of IA6, the method of averaging the integral value of the six methylene carbon atoms in IA6 was adopted for the exactness of integration, i.e.:

$$I_{\text{IA6}} = (I_{\text{C-1}} + I_{\text{C-2}} + I_{\text{C-3}})/6 = 4.80$$

The monomeric unit of HBA has three connecting

manners with other monomers to form I-H, H-D, and H-H dias sequences. The last two sequences are integrated together because it is difficult to distinguish them strictly in the ^{13}C -NMR spectrum for the analogy of chemical structures between HBA and DHBP. Carbon atoms C-12 and C-12' in HBA are chosen for integration, representing monomeric unit HBA in respect that the C-13 and C-14 in HBA overlap respectively, with C-18 and C-19 in DHBP, i.e.:

$$I_{\text{I-H}} = I_{\text{C-12}} = 3.77$$

$$I_{\text{H-H(D)}} = I_{\text{C-12'}} = 6.17$$

For one C-12 or C-12' represents only one HBA monomeric unit, so:

$$I_{\text{HBA}} = I_{\text{I-H}} + I_{\text{H-H(D)}} = 9.94$$

For the monomer unit of DHBP, it has only two connecting manners with other monomeric units as H-D and I-D. For the same reason as above, C-17 and C-17' were chosen for integration representing DHBP, i.e.:

$$I_{\text{H-D}} = I_{\text{C-17}} = 5.86$$

$$I_{\text{I-D}} = I_{\text{C-17'}} = 4.06$$

For two C-17 or C-17' represents one DHBP monomeric unit, so:

TABLE I Summarization of the Peak Assignments and Integration Values of Carbon Atoms in PEIK(F)		
Carbon no.	Chemical shift (ppm)	Integration value
1	28.01	10.00
2	29.85	9.36
3	40.89	9.41
4	172.25	19.79
5	136.88	9.67
6	127.61	9.70
7	134.10	10.03
8	139.43	10.39
9	126.51	10.49
10	138.12	9.33
11	167.60	9.13
12	157.90	3.77
13,13',18	123.95–124.47	45.92
14,19	134.82	41.31
15	129.03	6.38
16	169.44	5.58
17	157.18	5.86
20	137.07	5.79
21,21'	202.29–202.55	4.17
12'	157.56	6.17
14'	134.57	3.56
15'	128.80	3.85
16'	169.56	3.75
17'	156.84	4.06
20'	137.23–137.29	3.95

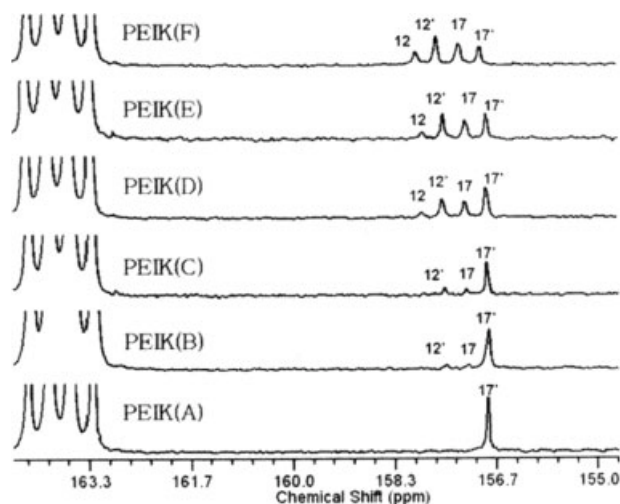


Figure 6 ^{13}C -NMR spectra (inverse gated decoupling) of PEIK(A–F) dissolved in CF_3COOD (multiple peaks around 163 ppm belong to solvent CF_3COOD).

$$I_{\text{DHBP}} = (I_{\text{H-D}} + I_{\text{I-D}})/2 = 4.96$$

At last, the integration of HBA-HBA sequence is obtained as:

$$I_{\text{H-H}} = I_{\text{H-H(D)}} - I_{\text{H-D}} = 0.31$$

Summing up the analyses, an exciting result is drawn that the monomer unit ratio shows IA6 : HBA : DHBP = 4.80 : 9.94 : 4.96, which is very close to the original monomer addition ratio 1 : 2 : 1. The sequence ratios of I-H, H-D, I-D, and H-H could also be decided by the method described above as I-H : H-D : I-D : H-H = 3.77 : 5.86 : 4.06 : 0.31.

As illustrated earlier, the integration method was also adopted to determine other monomeric unit ratios and sequence distributions in PEIK(A–E). Figure 6 shows the full range of ^{13}C -NMR spectra (inverse gated decoupling) of PEIK(A–F) dissolved in CF_3COOD .

Table II lists the ratios and molar fractions of the monomer units in the PEIKs samples. The HBA addition molar fractions range from 33% to 50% for PEIK(D–F) do greatly accord with the calculating integral values. But compared with those of PEIK(B–C), the calculating integral values departed correspondingly from their monomer feeding ratios. It is probably because the peak signals of the carbon atoms in the HBA monomer units, which are much weaker in PEIK(B–C), affect the exactness of integration with the reduction of HBA feeding ratio. At the beginning, the error of integration is not so significant to affect the calculation value. However, when the addition molar fraction of HBA drops down

below 20%, the integration errors became more considerable as for those of PEIK(B–C).

From the results of sequence distributions for PEIK(A–F), as shown in Table III, it can be found that the sequence ratios of I-H, H-D, and H-H increase with the rising of HBA molar fraction in the copolymers. In contrast, the sequence ratios of I-D decrease. It is worth noting that the sequence ratios of H-H are always very small ranging only from 0% to 2.21% in total amount of the four sequences for PEIK(A–F), indicating that few HBA monomer was self-polymerized in these reaction systems.

In the copolymers, sequences I-H and I-D can be classified as soft chain sequences because monomer IA6 contains a flexible “spacer” of six methylene groups. Similarly, sequences H-D and H-H can be classified as rigid chain sequences because monomer HBA and DHBP are all consisted of rigid aromatic structures connected by ester groups. Interesting results are found from the investigations on the rigid and soft character of the chain sequences. With the increase of fed HBA molar fraction changing from 0 to 50%, the fraction of soft sequences in the copolymers decreases from 100% to 55.93%, accordingly the fraction of rigid sequences increases from 0% to 44.07%. As for the soft sequences, the fraction of sequence I-H is 0% for PEIK(A–C), and increases up to 26.93% for PEIK(D–F). With this “three-step-feeding” procedure, we anticipated monomer IA6 would fully react with HBA in the first two steps. However, the results show that the IA6 monomers had only been partially reacted under these experimental conditions, although the fraction of I-H sequences exhibits an uptrend with increasing HBA molar fraction. In contrast, the fraction of sequences I-D reduces by 71% from 100% down to 29% for all the copolymer samples, which is indicative of more reactive of IA6 with monomer DHBP than it is with

TABLE II
Monomeric Unit Ratios and Mole Molar Fractions for PEIK(A–F) Determined by Integration from the NMR Spectra

PEIK (HBA mol %)	IA6		HBA		DHBP	
	Ratio ^a	mol % ^b	Ratio	mol %	Ratio	mol %
A (0)	5.02	52.95	0	0	4.46	47.05
B (10)	4.95	50.30	0.58	5.89	4.31	43.80
C (20)	4.92	43.66	1.58	14.02	4.77	42.32
D (33)	4.91	33.18	5.04	34.05	4.85	32.77
E (40)	5.13	31.11	6.50	39.42	4.86	29.47
F (50)	4.80	24.37	9.94	50.46	4.96	25.18

^a The ratio here means the monomer ratio calculated from the original integral value with referred integration method in the previous section.

^b mol % means the molar fraction of different monomeric unit in PEIKs with varied HBA content.

TABLE III
Sequence Distribution of Samples PEIK(A–F) Determined by Integration from the NMR Spectra

PEIK (HBA mol %)	I-H		H-D		I-D		H-H	
	Ratio ^a	mol % ^b	Ratio	mol %	Ratio	mol %	Ratio	mol %
A (0)	0	0	0	0	8.92	100	0	0
B (10)	0	0	0.60	6.96	8.02	93.04	0	0
C (20)	0	0	1.57	16.25	7.96	82.40	0.13	1.35
D (33)	1.02	9.32	3.79	34.64	5.90	53.93	0.23	2.10
E (40)	1.59	13.77	4.66	40.35	5.05	43.72	0.25	2.16
F (50)	3.77	26.93	5.86	41.86	4.06	29.00	0.31	2.21

^a The ratio here means the ratio of sequences calculated from the original integral value with referred integration method in the previous section.

^b mol % means the molar fraction of different sequence in PEIKs with varied HBA content.

HBA. On the basis of the data in Table III, as more HBA was added, the molar fraction of H-D sequence in the as-synthesized PEIK molecules increased first, and reached the maximum as the content of HBA added was 40 mol %. For the I-H sequence, it started to emerge in the molecules as 33 mol % of HBA were added, and continue to increase upon adding HBA. Along this line, the HBA monomers seemingly more prefer to react with DHBP monomers than IA6 monomers and DHBP have a superiority to react with IA6 in the competitive reaction with HBA, which can be supported by Figure 7 also. Therefore, the “step-feeding” method in this work may be utilized as a good strategy to acquire poly(ester imide ketone)s with controlled chain composition and sequence structures, which was not achievable by the “mixed-feeding” method adopted by Chi in the previous work.¹² As for all the samples of PEIK(A–F), the fraction of rigid sequences H-H increases only up to 2.21%, suggesting that monomer HBA is difficult to self-polymerize. Consequently, the H-D sequences (increased by 41.86%), which dominate the content of rigid sequences, should play a significant role in affecting the properties of these liquid crystalline copolymers.

Observation by polarized light microscopy

Figure 8 shows the typical polarized-light microscope morphologies obtained after the PEIK(D–F) samples were sheared on the slide at a temperature slightly below the liquid crystalline transition temperature. It is evident that typical banded textures, the characteristic of main chain nematic liquid crystalline polymers,¹⁴ can be observed in PEIK(D–F), of which the bands are perpendicular to the shearing direction. However, samples PEIK(A–C) display no orientation or characteristic texture of nematic mesophase.

From the analyses in the previous sections, it can be confirmed that the HBA content strongly affects the liquid crystalline birefringence. Samples PEIK(A–C) do not show any nematic mesophase, whereas

samples PEIK(D–F) with higher HBA content exhibit clear banded nematic textures. It is well known that the length of aliphatic spacer and the mesogenic character of the rigid unit affect considerably the mesophase morphology of the semiflexible liquid crystalline polymers.^{15–18} As an important mesogenic unit, the HBA monomer content in the copolymers determines the length of rigid mesogenic units with fixed fraction of spacers. When the HBA content is less than 33 mol %, the soft sequences are in dominance, resulting in the shorter length of rigid-rod mesogen. With the increase of HBA molar fraction, the fraction of rigid sequences is enhanced as identified by the NMR results, and the length of rigid mesogenic units increases.

Upon stepwise increasing the temperature, the transition processes from the solid to the nematic and then to the isotropic state could be clearly observed. Figure 9(a) shows a distinct nematic threaded texture of sample PEIK(F) at 330°C upon first heating. The clear-cut threaded texture and banded texture sheared in the molten state are direct evidence for the existence of nematic mesophase

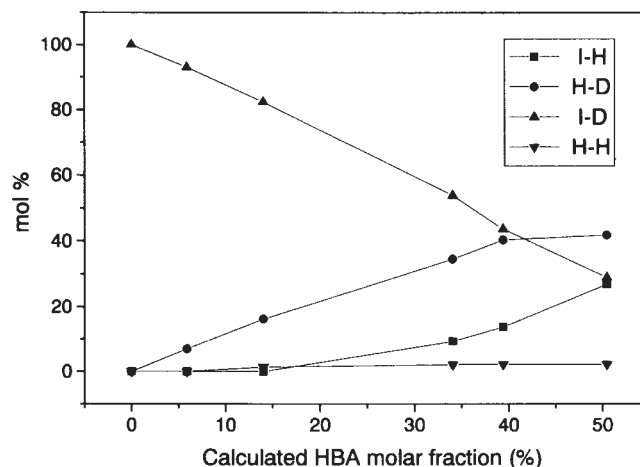


Figure 7 Plot of HBA molar fractions against the molar fractions of four sequences calculated from the integration of NMR spectra.

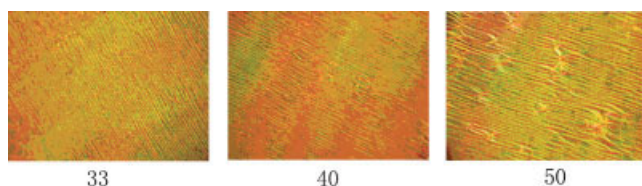


Figure 8 Polarizing microscope photographs of PEIK(D–F) with different HBA molar fraction at sheared state ($\times 500$). [Color figure can be viewed in the online issue, which is available at www.interscience.wiley.com.]

upon heating. But this threaded texture could not be found again upon subsequent cooling after heating the specimen over the isotropic transition temperature, indicating that the PEIK(F) copolymer does not belong to the common monotropic liquid crystalline polymer.¹⁹ When the temperature was raised to 360°C, it was observed that the birefringence of the polymers completely disappeared. However, with the increase of temperature, birefringence was present again and not observed until the sample neared to decompose as shown in Figure 9(b). Then, the liquid crystalline polymer entered the isotropic state. Usually, the main chain liquid crystalline polymers with distinct banded nematic texture would be processed in relative ease to form fibers, and we do find samples PEIK(D–F) possessing excellent fiber forming ability. It is our belief that these poly(ester imide ketone)s should be the suitable polymers of high performance fiber and fiber modification materials.

Wide-angle X-ray diffraction

Figure 10 shows the wide-angle X-ray diffraction (WAXD) patterns of powder samples of PEIKs as synthesized. There are at least two reflections at low angles ($2\theta < 12^\circ$) for PEIKs(A–C), which should correspond to the first- and second-order reflections of a layer spacing in the ordered structures. At higher angles ($2\theta > 12^\circ$), there are three distinct reflections which should be associated with the lateral packing order, as suggested by Kricheldorf and coworkers.²⁰

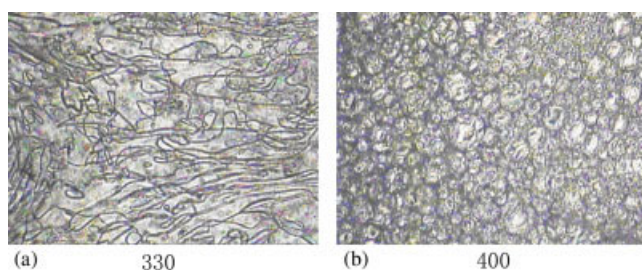


Figure 9 Polarized microscope photographs of melting process of PEIK(F) ($\times 500$). (a) nematic threaded texture formed at 330°C; (b) birefringence formed at 400°C. [Color figure can be viewed in the online issue, which is available at www.interscience.wiley.com.]

As the imide groups are highly polar, the dispersion of the alkane phase in their molecules is, of course, energetically highly unfavorable. This allows the interpretation of a phase separation on the nanometer level.¹⁶ From this point of view, it is clear that the reflections at low angles are associated with the layer structures packed by the spacer units, and those reflections at higher angles should be associated with the ordered structures packed by rigid mesogenic units. With the increase of HBA content, the proportion of flexible spacers in PEIKs is slowly decreased. This well agrees with the explanation that the increase in the length of rigid mesogenic units hampers the packing of alkane spacers in the layers in response to the gradual diminishment of intensity for the small angle reflections, indicating the disappearance of layer structure in PEIK(D–F) as shown in Figure 10.

Decline in the crystallinity is found with increasing the HBA content and rigid sequences. This trend is also generally found in the semiflexible liquid crystalline polymers with the increased length of rigid mesogenic units, suggesting that the mobility of mesogen strongly influences the process of crystallization.²⁰

DSC measurements

All the as-synthesized PEIKs powders were subjected to DSC measurement at a heating and cooling rate of 20°C/min in the range of 40–300°C, as shown in Figure 11.

In the DSC traces, the nematic-to-isotropic transition temperature (T_i) seems not detectable, but it can be clearly observed by polarized light microscopy. The glass transition temperatures (T_g) can be observed in the second heating runs. The T_g and T_m

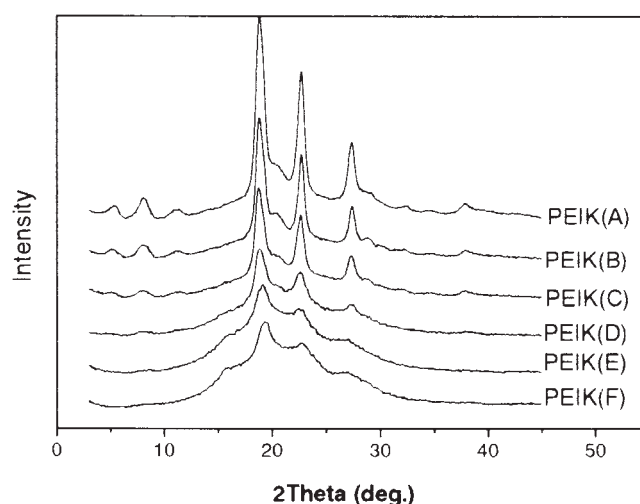


Figure 10 WAXD patterns of as-synthesized PEIKs.

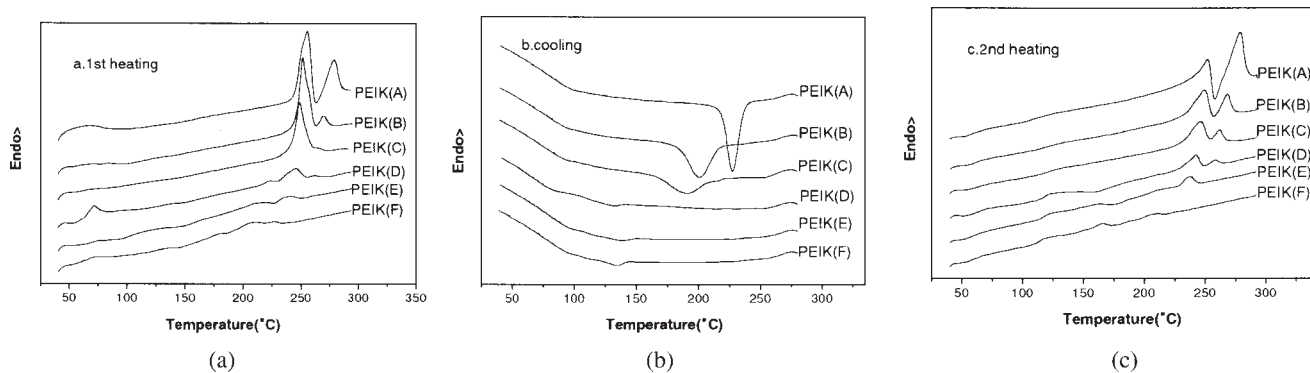


Figure 11 DSC measurements of PEIKs with heating and cooling rate of 20°C/min. (a) first heating; (b) cooling; (c) second heating.

values taken from the first and second heating scans are listed in Table IV.

In the cooling curves [Fig. 11(b)], samples with lower HBA content, PEIK(A–C), exhibit one exothermic peak of crystallization, and it becomes broader upon increasing the HBA content in the molecules. Moreover, the transition temperature of crystalline peak also decreases. Whereas those with higher HBA content, PEIK(D–F) exhibit no exothermic peak, indicating that high HBA content and molar fraction of rigid sequences does not favor the crystallization but facilitate the formation of mesogenic phase.

Comparing the first heating curves [Fig. 11(a)] with the second one [Fig. 11(c)], for PEIK(A–C), an apparent decrease of the first endothermic peak following the growth of the second endothermic peak is clearly observed. However, for PEIK(D–F), which have higher HBA content in the molecules, this change is more reluctant to happen and also the second endotherm gradually disappears. With the observation of the exothermic changes upon cooling, this reorganization process can be explained as that, a new ordered phase after the melting of the origin

ordered phase, which is able to grow up during cooling, is formed. And, as the HBA content in the molecules is increased, the reorganization process is hindered and the growth of the new ordered phase becomes more difficult. This speculation also can be supported by the WAXD experiment. The reflections at low angle of 3°–12°, for sample PEIK (D–F), cannot be observed, which are reversely more apparent for PEIK(A–C). Because the reorganization process leads to the formation of a new order phase, which consequently causes the second endotherm for PEIK(A–C), it is reasonable to consider those low angle reflections actually referred to the existence of the new ordered phase mentioned above. Therefore, the WAXD patterns of PEIK(A–C) are considered to be attributed to the coexistence of two different ordered phases, which gives the observed two endothermic transitions during both heating in DSC experiments.

For most poly(ester imide)s with liquid crystalline characters, these two endothermic transitions are believed to be indicative of the transition from the solid state to the smectic phase or nematic phase, and to the

TABLE IV
Transition Temperatures of PEIKs with Different Heating Procedures

Procedure	HBA molar fraction (mol %)	T_g (°C) ^a	T_{m1} (°C)	T_{m2} (°C)	T_{m3} (°C)	T_i (°C) ^b
1st heating	0	–	256.0	278.9	–	–
	10	–	252.0	270.3	–	–
	20	–	249.1	–	–	–
	33	–	223.8	245.9	262.3	310–320
	40	–	219.8	240.9	–	355–365
	50	–	211.1	227.7	–	400–410
2nd heating	0	112.3	252.2	279.0	–	–
	10	118.3	249.6	268.6	–	–
	20	119.2	246.6	261.9	–	–
	33	119.4	242.8	258.3	–	–
	40	118.6	237.5	–	–	–
	50	114.7	211.0	–	–	–

^a T_g is only detectable in the second heating curves.

^b T_i is observed by polarized light microscope.

TABLE V
Dependence of TGA Data on HBA Molar Fraction

PEIKs (HBA mol %)	A(0)	B(10)	C(20)	D(33)	E(40)	F(50)
Temperature (°C) (weight loss 5%)	408.1	414.8	412.5	425.5	433.1	435.2
Temperature (°C) (max decomposed rate)	474.7	475.5	476.5	488.6	484.2	494.7
Percentage (%) (residual mass)	1.07	2.64	2.65	1.87	0.63	1.27

isotropic phase, respectively. Nevertheless, in an earlier report of Chi et al.,¹² a model was proposed to illustrate that the two endothermic transitions of the similar PEIKs could be referred to the transitions from the three-dimensional solid state to the two-dimensional smectic transient phase and the two-dimensional phase to the one dimensional nematic liquid crystalline phase, respectively. In this experiment, this model fits quite well for samples PEIK(D–F), but is not adequate for the transitional behaviors for samples PEIK(A–C) with no mesophase transition in melting. The details of phase transitions for samples PEIKs(A–C) still need further study.

It is well known that the length of aliphatic spacer unit and mesogenic character of rigid unit affects the stability of mesophase in the semiflexible liquid crystalline polymers.¹⁹ Although the methylene units in the semiflexible liquid crystalline polymers would participate in the ordering of a mesophase, their thermodynamic contributions are known to be lower than those of mesogenic units. As a result, the lower the fraction of the methylene spacer in the copolymers such as PEIK(D–F), the higher the mesophase to isotropic phase transition temperature as identified by polarized light microscopy. It is evident that the decline of crystallization temperature exhibits an apparent alleviation for PEIK(D) and the crystallization peak begin to obscure in the curve and last vanish for PEIK(F).

The glass transition temperatures T_g of the PEIK samples can be determined with care from the sec-

ond heating curves of DSC measurements, as shown in Figure 11(c). It may be found that the T_g transition increases by adding HBA units into the polymers, but slightly drops down for samples with high molar fraction of HBA, indicating that the enhancement of molecular chains' rigidity lowers their mobility, but increases the fraction of amorphous section as identified by WAXD.

In respect that a "step-feeding" polycondensation method was adopted in this experiment, PEIKs with controlled sequence structures would be acquired. The above thermal analysis results suggest that copolymers with designed chain composition and sequence structures can be obtained, which provides an useful means for studying the relationship of sequence structure and properties of PEIK polymers.

TGA measurement

The thermal stability of the PEIK samples was evaluated by TGA, which was performed in air at a heating rate of 20°C/min. The TGA curves of the copolymers with different HBA molar fractions are shown in Figure 12. The decomposition temperature for 5% weight loss, which indicates the onset of significant thermal degradation of polymers, ranges from 408°C to 435°C. Relative data is shown in Table V. By and large, the decomposition temperature for 5% weight loss and the decomposition temperature for maximum decomposed rate gradually rise with the increase of HBA molar fraction. As the rigid sequences are mainly consisted of benzoic "rigid" building block, their thermal stability is so fine that they do not decompose at high temperature. However, those soft sequences are consisted of both benzoic "rigid" and methylene "soft" building blocks, and become the weak segments which often lead to the first breakage of the molecular chain. From the residual mass of the TGA experiments, all the PEIK samples are almost decomposed completely, suggesting that the copolymers synthesized in this study contain no, if any, prolonged rigid benzoic blocks in the chain sequence structure.

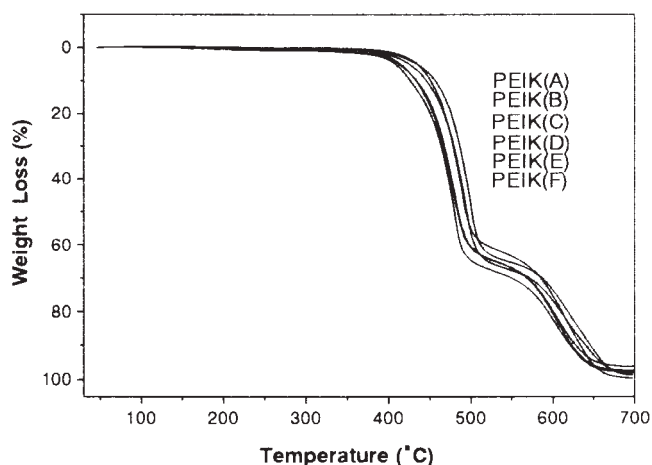


Figure 12 TGA curves of polymers with different molar fractions of HBA.

CONCLUSIONS

A series of PEIKs with various HBA molar fraction were synthesized by a "step-feeding" polycondensation method. It was verified by the NMR studies that

the HBA and other monomeric unit ratios in the PEIKs are very close to the ratios of the monomers added into the polycondensation systems. The sequence ratios of I-H, H-D, and H-H increase with increasing the HBA content, while that of I-D decrease. The sequence ratios of H-H detected are always very small when compared with others, indicating that monomer HBA is difficult to self-polymerize in the polycondensation conditions. With this "step-feeding" method, poly(ester imide ketone)s with controlled chain composition and sequence structures as well as designed properties can be acquired, and it will be helpful for detailed investigation of the relationship of sequence structure and properties of PEIK polymers.

Some of the PEIK samples synthesized in this work exhibit typical characteristics of nematic main chain liquid crystalline polymers. Significant banded textures and threaded texture can be observed in the sheared state and molten state, respectively for PEIK(D-F) samples with higher HBA content. This may be due to the changes in the length of rigid mesogenic units in PEIKs. Additionally, it is found that samples PEIK(D-F) possess good thermal stability, moderate melting temperature, and excellent fiber-forming ability, which make these polymers to be suitable polymers as high performance fiber and fiber modification materials.

References

1. Kricheldorf, H. R.; Pakull, R. *Polymer* 1987, 28, 1772.
2. Kricheldorf, H. R. *Adv Polym Sci* 1999, 141, 83.
3. Kricheldorf, H. R.; Pakull, R.; Buchner, S. *Macromolecules* 1988, 21, 1929.
4. Kricheldorf, H. R.; Schwarz, G.; de Abajo, J.; de la Campa, J. G. *Polymer* 1991, 32, 942.
5. Kricheldorf, H. R.; Schwarz, G.; Domschke, A.; Linzer, V. *Macromolecules* 1993, 26, 5161.
6. Nieri, P.; Reddy, C. R.; Wu, C. N.; Munk, P.; Lenz, R. W. *Macromolecules* 1992, 25, 1796.
7. Ignatious, F.; Lenz, R. W.; Kantor, S. W. *Macromolecules* 1994, 27, 5248.
8. Hsu, T. F.; Lin, Y. C.; Lee, Y. D. *J Polym Sci Part A: Polym Chem* 1998, 36, 1791.
9. Higashi, F.; Akiyama, N.; Takahashi, I.; Koyama, T. *J Polym Sci Polym Chem Ed* 1984, 22, 1653.
10. Higashi, F.; Mashimo, T. *J Polym Sci Polym Chem Ed* 1985, 23, 2999.
11. Higashi, F.; Mitaani, K. *J Polym Sci Part A: Polym Chem* 2000, 38, 1270.
12. Chi, Z. G.; Xu, J. R. *J Appl Polym Sci* 2003, 90, 1045.
13. Stanley, L. N. U.S. Pat. 3,073,866 (1963).
14. Tong, Y. J.; Guan, H. M.; Li, X. R.; Dong, D. W. *Chem Res* 1999, 10, 7.
15. Kricheldorf, H. R.; Schwarz, G.; Berghahn, M.; de Abajo, J.; de la Campa, J. *Macromolecules* 1994, 27, 2540.
16. Kricheldorf, H. R.; Probst, N.; Schwarz, G.; Wutz, C. *Macromolecules* 1996, 29, 4234.
17. Kricheldorf, H. R.; Linzer, V.; Leland, M.; Cheng, S. Z. D. *Macromolecules* 1997, 30, 4828.
18. Paradey, R.; Shen, D. X.; Gabori, P. A.; Harris, F. W.; Cheng, S. Z. D.; Adduci, J.; Facinelli, J. V.; Lenz, R. W. *Macromolecules* 1993, 26, 3687.
19. Kim, S. O.; Koo, C. M.; Chung, I. J.; Jung, H. T. *Macromolecules* 2001, 34, 8961.
20. Leland, M.; Wu, Z. Q.; Ho, R. M.; Cheng, S. Z. D.; Kricheldorf, H. R. *Macromolecules* 1998, 31, 22.